Separation and Purification Technology 244 (2020) 116427

Contents lists available at ScienceDirect

Separation and Purification Technology

journal homepage: www.elsevier.com/locate/seppur

Post-combustion CO_2 capture and recovery by pure activated methyldiethanolamine in crossflow membrane contactors having coated hollow fibers

Aytac Perihan Akan[a,b], John Chau[a], Kamalesh K. Sirkar[a,*]

[a] Otto H. York Department of Chemical and Materials Engineering, Center for Membrane Technologies, New Jersey Institute of Technology, Newark, NJ 07102, USA
[b] Department of Environmental Engineering, Hacettepe University, Ankara 06800, Turkey

ARTICLE INFO

Keywords:
Post-combustion CO_2 capture
Membrane contactor
Hollow fiber membrane
Absorption and stripping
Pure methyldiethanolamine/piperazine

ABSTRACT

Gas absorption and stripping using membrane contactors is one of a number of carbon capture and storage technologies being investigated for separating CO_2 from flue gas. Energy consumption in CO_2 absorption-stripping employing amine-containing aqueous absorbent solutions is strongly influenced by demanding stripping conditions involving higher temperatures. The utility of using pure methyldiethanolamine (MDEA) activated by piperazine as a reactive absorbent was studied using a compact hollow fiber device for the absorber as well as the stripper. Water needed for reactive absorption of CO_2 in tertiary amine MDEA was obtained from simulated humidified flue gas stream which is saturated with moisture in actual practice. This study investigated also the absorption and stripping performances of aqueous absorbent solutions containing 80% and 90% activated MDEA (aMDEA). Considerable CO_2 stripping from CO_2-loaded pure aMDEA absorbent was achieved at 92 °C while absorption was carried out at 25–46 °C. Further, the CO_2 stripping rate was far higher for pure MDEA compared to the other two aMDEA solutions with water. Results are reported for the performance of the absorption-stripping process as a function of humidified simulated flue gas flow rate and the absorbent flow rate. High values of the overall mass transfer coefficients (MTCs) have also been reported for absorption. The highest volumetric gas phase based overall MTC obtained was 0.504 sec^{-1}. This system has a much lower absorbent circulation load, eliminates the energy needed to heat and evaporate water present in aqueous absorbent solutions and benefits from the absence of excess water during stripping.

1. Introduction

Rapid growth of human population and advances in industry and related anthropogenic activity leading to greenhouse effect from burning of fossil fuels among others is a leading cause of global warming. The release of high concentrations of greenhouse gases (GHGs) such as carbon dioxide (CO_2), nitrous oxide, chlorofluorocarbons (CFCs) and methane (CH_4) to the atmosphere as a result of human activities has been shown to be the fundamental reason for global warming leading to increasing atmospheric temperature, rising sea levels and melting glacier [1–8]. Burning coals for power generation is one of the primary sources releasing CO_2 emissions into the atmosphere [8,9]. The increase in GHGs depending on energy consumption is expected to increase by approximately 30% by 2040 [9].

To mitigate CO_2 emissions into the atmosphere, a variety of technical methods are being explored as part of carbon capture and storage (CCS) technologies [10,11] including use of non-fossil fuel power sources, improvements in energy efficiency and thereby decreasing the energy demand [2,12]. Technologies proposed for CO_2 separation and capture from pre-combustion and post-combustion systems include [13,1,5]: Absorption, adsorption, cryogenic distillation and membrane processes [3,13,14]. Membrane-based absorption is being increasingly studied in membrane contactor configuration due to its many potential advantages [15,16]. Most membrane contactor studies have focused on gas absorption; relatively few have focused on stripping. However, there are other aspects crucial for drastically reducing cost of membrane contactor-based processes. These involve energy cost for stripping/regeneration, absorbent selection, absorbent circulation load, membrane device cost etc.

An important source of energy expenditure in CCS process via absorption involves the cost of absorbent regeneration. In systems involving a primary amine such as monoethanolamine (MEA), the stripping

* Corresponding author.
E-mail address: sirkar@njit.edu (K.K. Sirkar).

https://doi.org/10.1016/j.seppur.2019.116427
Received 22 October 2019; Received in revised form 13 December 2019; Accepted 13 December 2019
Available online 15 December 2019
1383-5866/

Notation

a_v	Membrane surface area per unit volume, m^{-1}
A_m	Membrane area, m^2
C	Concentration, mol/cm^3
$C_{CO_2,g,in}$	Concentration of CO_2 in the gas stream inlet, $gmol/cm^3$
$C_{CO_2,g,out}$	Concentration of CO_2 in the gas stream outlet, $gmol/cm^3$
K_{og}	Overall gas film-based mass transfer coefficient, m/s
N_{CO_2}	Molar flux of CO_2, $gmol/m^2$-s
P_t	Total pressure, atm
Q_g	Inlet feed gas flow rate, cm^3/min
R	Gas constant, cm^3-atm/K-gmol
T	Temperature, K
$y_{CO_2,g,in}$	CO_2 mole fraction at absorption module inlet
$y_{CO_2,g,out}$	CO_2 mole fraction at absorption module outlet
y^*_{in}	Hypothetical inlet gas phase mole fraction in equilibrium with liquid phase
y^*_{out}	Hypothetical outlet gas phase mole fraction in equilibrium with liquid phase

Greek letters

Δy_{lm}	Logarithmic mean mole fraction

Superscripts and subscripts

t	total

temperature is quite high 110–120 °C at ~2 atm for feed flue gas at ~40–50 °C [17]. Further, the solution contains ~30% MEA in water. Therefore, the heating energy input at a high temperature requires one to heat up and evaporate the water as well. Conditions are not very different if an aqueous solution of a tertiary amine, methyldiethanolamine (MDEA) is used. For example, Li et al. [18] employed 40–50 wt% MDEA containing a small amount of activator, piperazine (PZ), in water as absorbent and a first stage stripping temperature of 119–128 °C with a trans-membrane pressure drop of ~60 psi during regeneration.

The membrane material in the module is also important. Li et al. [18] employed highly hydrophobic microporous hollow fiber membranes of polyetheretherketone (PEEK) a polymer that is order/s of magnitude costlier than conventional membrane contactor polymers like polyvinylidene fluoride (PVDF), polypropylene (PP) etc. It is possible to have relatively inexpensive surface modification of polymers like PP and PVDF to endow them with very high hydrophobicities [19] to prevent pore wetting. Employment of appropriate cross-flow hollow fiber module design can also ensure high liquid-phase mass transfer coefficients.

The chemistry of CO_2 absorption is quite important for efficient CO_2 stripping as well. The absorption of CO_2 by MDEA, a tertiary amine, needs the presence of water:

$$R_1R_2R_3N + CO_2 + H_2O \overset{k_{2,Amine}}{\leftrightarrow} R_1R_2R_3NH^+ + HCO_3^- \quad (1)$$

It is a base-catalyzed hydration of CO_2 forming a protonated amine and a bicarbonate anion [20]. Addition of small amounts of other non-tertiary amines such as piperazine and creating an activated solution, aMDEA, to enhance the rate requires additional considerations (see Cao et al. [21] for additional references). In flue gas absorption process, the flue gas is saturated with moisture. Therefore, in a possible scenario, the tertiary amine absorbent does not need to have any water since it will come from the flue gas itself. Correspondingly, during stripping if the absorbent is pure amine-based without any water, any loss of moisture due to stripping conditions will also facilitate CO_2 stripping during the reversible reaction (1). This will reduce the volume of circulating absorbent liquid, eliminate heat utilized to evaporate the water as well as potentially create conditions for lower temperature desorption of CO_2; these are important in making the process highly energy efficient. Yet most of the studies in literature employed aqueous solutions of MDEA [18,21–27]. Thus, studies with pure aMDEA is a major goal of this study. However, it also raises the possibility of pore wetting of microporous hydrophobic membranes since the absence of water decreases the surface tension of the polar organic absorbent and increases the possibility of membrane pore wetting in PP hollow fiber membranes. Therefore, the hollow fibers here had a porous fluorosiloxane coating on the outside surface exposed to the absorbent.

In this study, we have investigated CO_2 absorption from a simulated humidified flue gas stream into an activated MDEA absorbent solution where water content was varied between 20% and 0%, the last one corresponds to pure MDEA; the activator was piperazine (PZ). The rectangular membrane modules for absorption-stripping were small crossflow porous hollow fiber membrane (HFM) devices built using PP HFMs whose outside surface had a light plasma polymerized fluorosiloxane coating. The effects of a variation in the flow rate of simulated flue gas, absorbent liquid flow rate and stripping conditions were investigated. CO_2 mass transfer coefficients were estimated; the corresponding volumetric mass transfer coefficients were calculated. These have been compared with the available information from literature.

2. Materials and methods

2.1. Materials

2.1.1. Membranes and modules

Hollow fiber membrane contactors employed microporous hydrophobic polypropylene (PP) hollow fibers. The rectangular open picture frames containing the hollow fiber membranes were developed by Applied Membrane Technology (Minnetonka, MN). The dimensions and properties of the hollow fibers are provided in Table 1. The outside surface of the hollow fibers had a thin plasma polymerized porous hydrophobic coating of fluorosiloxane. For the stripping modules, the coating was slightly thicker and therefore, the effective pore size was likely to be smaller. Correspondingly, the breakthrough pressure required at the liquid-gas interface is higher. This ensures liquid-gas phase interface stability since the stripping side liquid-gas interface is exposed to a significantly higher pressure difference due to the application of vacuum. JSM 7900F Field Emission SEM (JEOL USA, Peabody, MA) was used to take scanning electron micrographs (SEMs) of the plasma polymerized coated hollow fiber membrane surface.

The final module structure was prepared by backing up the open picture frame on both sides by first a flow distribution plate and then a face box (fabricated in-house); rubber gaskets were used in between

Table 1
Details of the cross-flow hollow fiber membrane modules.

*Hollow fiber ID (μm)	240
*Hollow fiber OD (μm)	290
Active fiber length (cm)	6.35
Fiber bed dimensions	2.5″ × 1″ × 3/4″
Fractional porosity of hollow fiber wall	0.40
Effective membrane surface area (cm^2)**	509
Number of hollow fibers	1064
Hollow fiber bed volume (cm^3)	61.7
Membrane surface area/bed volume, a_v (m^2/m^3)	2100
Membrane tortuosity	2.6
Average pore size (μm)	0.03

* Polypropylene hollow fiber with a light plasma polymerized coating on the fiber OD.

** Based on the fiber ID.

each flat plastic piece to prevent leakage. Nylon was used as the material of construction of the picture frame holding the hollow fibers; photos of various parts are shown in Mulukutla et al. [19]. One membrane module was used as the absorber and the other membrane module with a slightly thicker porous coating was used as the stripper.

2.1.2. Flue gas

Absorption and stripping experiments were carried out using a simulated flue gas mixture of composition 14.1% CO_2, 1.98% O_2 and balance N_2 (Airgas, Oakland, NJ, USA). In the experiments, this feed gas stream was humidified using a porous hydrophobic PP hollow fiber-based humidification module to mimic real flue gas in a power plant and to activate the reaction between methyldiethanolamine and CO_2 in the case of pure MDEA being used as the absorbent. In this study, the humidified feed gas was passed through the lumen side of the hollow fibers in the absorption module; the absorbent solution was introduced from the shell side of the membrane module in cross flow. In the stripping module, the CO_2-loaded absorbent solution was also introduced in cross flow over the hollow fibers. The absorption and stripping membrane contactors were filled with the absorbent solution before passing the feed gas.

2.1.3. Absorbent solution (activated methyldiethanolamine)

The absorbent liquid used was activated methyldiethanolamine (aMDEA) obtained by adding ~1% PZ to MDEA, 12.5 gm PZ to 1250 mL of MDEA. To obtain aqueous solutions, ultrapure water was used. Commercial MDEA used in all experiments was obtained from Fisher Scientific (IL, USA); PZ was procured from Sigma Aldrich (Milwaukee, WI, USA). Three solvent compositions tested in the current study were as follows: (1) 80 vol% aMDEA/20 vol% water, (2) 90 vol% aMDEA/10 vol% water, and finally (3) pure aMDEA. To prepare an aqueous absorbent including 80 vol% MDEA and 20 vol% water, MDEA

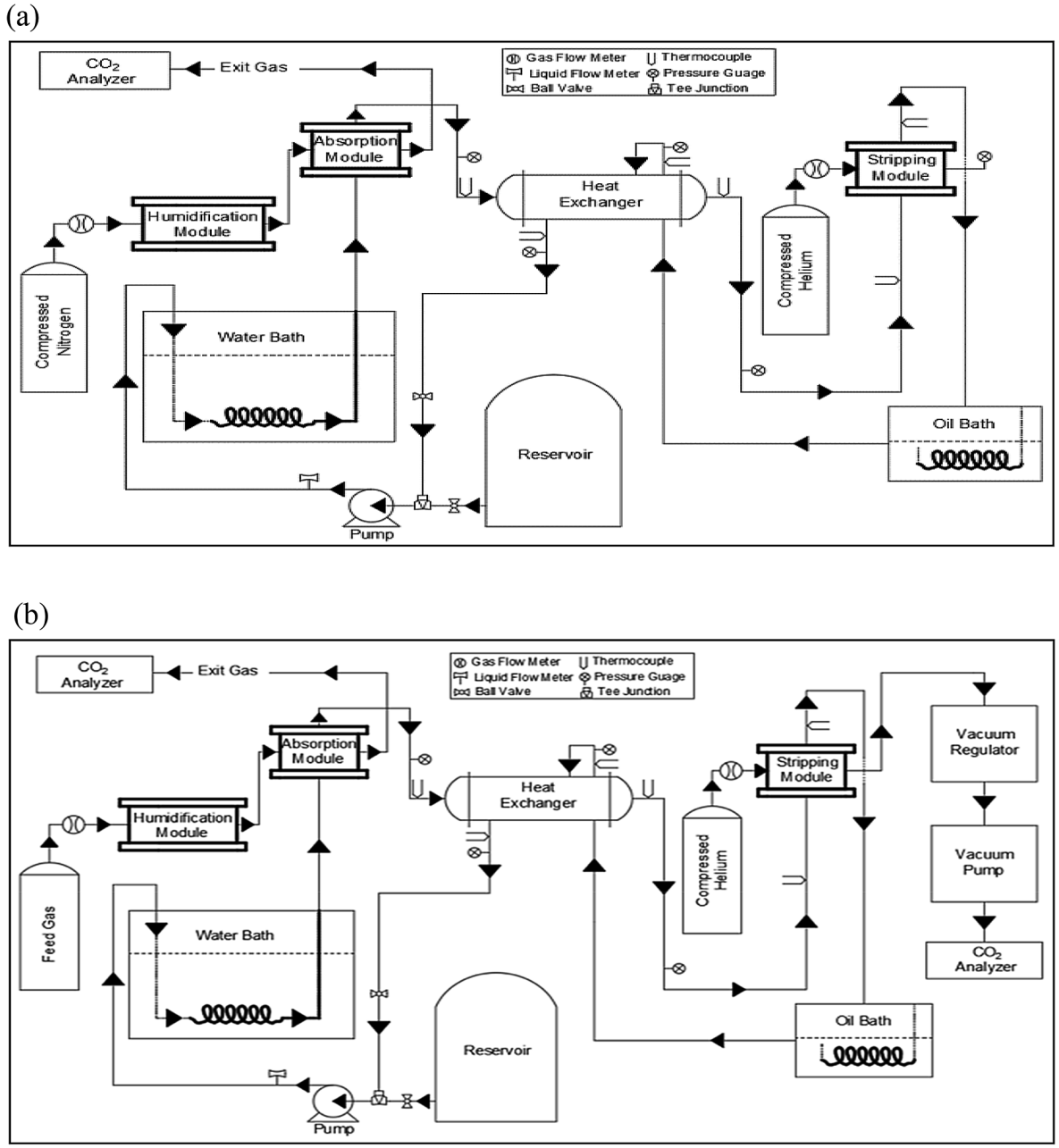

Fig.1. (a) Schematic diagram of the experimental setup with respect to feeding humidified N_2 gas before humidified feed gas into the lumen side of hollow fibers in absorption membrane contactor and (b) schematic diagram of experimental setup for startup (adapted from [19]).

of 800 mL was mixed with 200 mL of ultrapure water using a magnetic stirrer (Corning Hot Plate Stirrer, PC-351) in order to have a homogenous solution. For the preparation of an absorbent solution containing 90 vol% MDEA and 10 vol% water, 900 mL MDEA was mixed with 100 mL ultrapure water using a magnetic stirrer as in the case of 80 vol% MDEA. An appropriate amount of PZ was added to each of the above solutions to have a 1% composition.

2.2. Methodology

2.2.1. Experimental set up and procedure

The basic configuration of the experiment (Fig. 1a and b) involves pumping the absorbent liquid through the membrane absorber module to a heat exchanger (Model00256-03, Exergy LLC, Garden City, NY; supplied by Burt Process Equipment, Hamden, CT) where the CO_2-loaded absorbent can get heated up to 85–90 °C+. The heated up CO_2-loaded absorbent is then pumped to the shell side of the membrane stripping module. The stripped absorbent solution gets cooled somewhat; it is then sent to an oil bath for heating it up and then sending it to the heat exchanger where it heats up the CO_2-loaded absorbent exiting the membrane absorber. After cooling the spent absorbent substantially in the heat exchanger, it is either sent to a reservoir or to the membrane absorber module for CO_2 absorption. Simultaneously, humidified simulated flue gas is passed through the bores of hollow fiber membranes in the membrane absorber for CO_2 absorption. The spent CO_2 feed gas is sent through a solid-state IR-based CO_2 analyzer (Model 906, Quantek, Grafton, MA). On the strip side, helium gas was passed through the bore of the stripping module; the exiting gas containing stripped CO_2 in helium was subjected to controlled vacuum by a vacuum pump and a vacuum regulator. Its CO_2 concentration was measured by another Quantek CO_2 analyzer.

The first set of experiments were run with humidified N_2 gas flow rate of 50 cm^3/min and liquid absorbent with a liquid flow rate in the range of 15.10–18.90 L/h controlled by a liquid flow meter (1-GPI Model GM001S2C41-20.317 cm (1/8″) NPT s. steel oval gear meter, Great Plains Industries, Wichita, KS). This was done until the shell sides of both absorption and stripping membrane contactors were filled with the absorbent liquid. Then, sweep helium (Airgas, Oakland, NJ, USA) having a flow rate between 50 and 100 cm^3/min was introduced into the lumen side of hollow fibers in the stripping membrane contactor until liquid temperature entering the shell side of hollow fibers in the stripping module reached a minimum of 90 °C. This stage of the experimental procedure was the first stage illustrated in Fig. 1a.

During the second stage of experiments (Fig. 1b), humidified simulated flue gas mixture was introduced into the lumen side of hollow fibers in the absorption membrane contactor. Feed gas flow rate was controlled by a Multi-channel Mass Flow Controller (Model 8248A, Matheson TRI-GAS, Montgomeryville, PA, USA) and Mass Flow Controller Transducer (Model 8272-0452, Matheson TRI-GAS). Experiments were conducted with humidified feed gas flow rates of 50 cm^3/min, 100 cm^3/min, 150 cm^3/min, 200 cm^3/min, 250 cm^3/min and 300 cm^3/min and liquid flow rates of 15.10 L/h, 16.60 L/h and 18.90 L/h. A schematic diagram of the experimental set up for startup is shown in Fig. 1b. In the present study, the cooled CO_2-stripped liquid returning from the heat exchanger was not discharged to the reservoir; it was pumped directly to the absorption module.

Before starting a new set of experiments, the liquid absorbent to be placed in the reservoir was heated to 90 °C and stirred for 1 h on a hot plate magnetic stirrer (Corning Hot Plate Stirrer, PC-351) to obtain lean solvent from the absorbent with residual CO_2. Then a small amount of piperazine in the amount mentioned in Section 2.1.3 was added to the solution to provide activation of the liquid absorbent and the mixture was transferred to the reservoir for all studies in the new set of experiments. Mulukutla and coworkers [19] used a similar experimental setup to investigate CO_2 capture and recovery from simulated flue gas with or without moisture by using the ionic liquid [bmim][DCA] containing 20 wt% polyamidoamine [PAMAM] dendrimer Gen 0. Additional details on experimental procedure and equipment in the experimental setup and also schematic representations of both the absorbent flow around the fiber outside and the rectangular box arrangement are available in Mulukutla et al. [19].

2.2.2. Measurement of amine strength and regeneration test

The absorbent liquid was titrated with sulfuric acid (1 N) and methyl orange indicator to determine the working capacity of absorbent liquid and to check its concentration in the reservoir. Titration is the most commonly used method for amine strength determination. Amine strength is generally described as the amount of amine capable of reacting with acid gases. Titration for amine strength is a measure of the amount of base in the solution that is capable of reacting with acid gases expressed as the equivalent vol % of the amine primarily in use [28].

3. Results and discussion

In this study, a number of lab-scale CO_2 absorption-stripping experiments were implemented with different operating conditions, such as feed gas flow rate, liquid flow rate, and concentration of the aMDEA absorbent in water to determine the CO_2 absorption rate, CO_2 removal rate, percentage of CO_2 recovered, the overall gas-phase mass transfer coefficient for CO_2 absorption and the corresponding volumetric mass transfer coefficient.

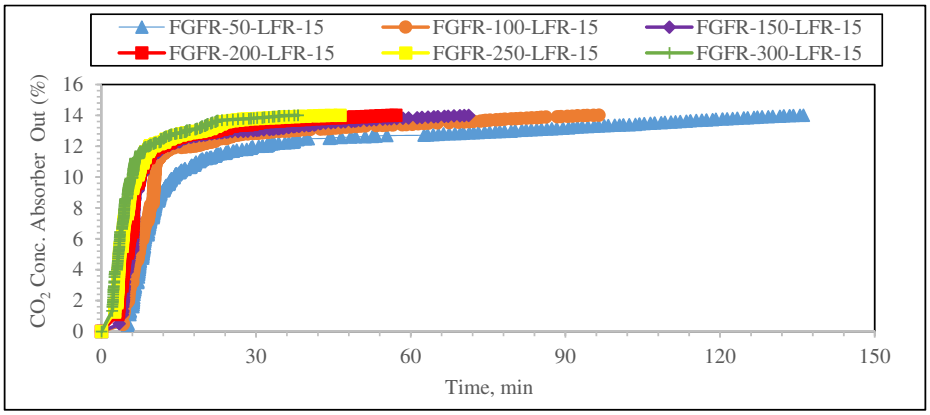

Fig. 2. CO_2 breakthrough results for aMDEA absorbent having 80 vol% aMDEA/20 vol% water at 15.10 L/h; the symbol FGFR-50-LFR-15 stands for: Feed gas flow rate (FGFR) at 50 cm^3/min and liquid flow rate (LFR) of 15 L/h.

3.1. Absorbent aMDEA concentration in water: 80 vol%, 90 vol%, 100%

In the first experiment, 80 vol% aMDEA liquid absorbent flow rate and sweep helium flow rate were respectively 15.10 L/h and 50 cm^3/min. Humidified feed gas flow rates into the lumen side of hollow fibers in the absorption module were varied between 50 cm^3/min and 300 cm^3/min for combo-mode stripping where the vacuum level applied was 1 in. Hg (2.54 cm Hg) and sweep helium flow rate was 50 cm^3/min. Feed gas and bed temperatures were 25 °C and 46.6 °C, respectively. Moreover, the liquid temperature entering stripping module was 102.4 °C. Fig. 2 shows CO_2 breakthrough results under these conditions.

Humidified feed gas flow rate of 50 cm^3/min showed the maximum CO_2 removal capacity in terms of percent of absorbed CO_2 which could be stripped out: the values were 6.85 cm^3/min for absorption and 5.72 cm^3/min of absorbed CO_2 being stripped for a % stripped as 83.5%. The rate of absorption was on the low side; correspondingly the absorbent liquid got saturated after 136 min, the longest time for this series of runs. For other gas flow rates between 100 and 300 cm^3/min, breakthrough times were 97, 71, 57, 46 and 38 min, respectively as seen in Fig. 2. On the other hand, for 300 cm^3/min feed flow rate, the rate of absorption was a high 38.3 cm^3/min while the stripping rate was very low at 1.63 cm^3/min; therefore, the percent of absorbed CO_2 that was stripped was very low at 4.26%. The CO_2 breakthrough results for 80% aMDEA absorbent at liquid flow rates of 16.60 and 18.90 L/h showed similar trends with respect to increasing gas flow rate. These results clearly show that the stripping being achieved in the absorption-stripping loop was insufficient. As a result, the concentration of the free amine available for absorption was gradually decreasing with time causing inadequate absorption-based removal of CO_2 from the feed gas. Finally, the absorbent became fully saturated at which time the feed gas did not undergo any further absorption and broke through the end of the absorber module.

Experiments with absorbent aMDEA at a concentration of 90 vol% (rest water) were also done under operating conditions very similar to those with the absorbent having 80 vol% aMDEA except for the absorption temperature (44.6 °C) and the stripping temperature (92.7 °C). The exiting concentrations from the absorber as a function of time are shown in Fig. 3. Corresponding to the increased humidified feed gas flow rates, the breakthrough times were 168, 105, 80, 64, 51 and 45 min, respectively (Fig. 3). When these breakthrough times are compared to those related to MDEA concentration of 80 vol% aMDEA/20 vol% water under same conditions, higher breakthrough times and higher absorption rates are observed due to the fact that higher concentration of amine brings about an increase in the absorption rate.

Experiments with pure absorbent aMDEA were done under operating conditions similar to those used with absorbent aMDEA at a concentration of 90 vol%. Fig. 4 shows CO_2 breakthrough results for a liquid flow rate of 15.10 L/h and sweep He flow rate of 50 cm^3/min in the case of pure aMDEA absorbent. Humidified feed gas flow rates in the range of 50–300 cm^3/min reached breakthrough at 214, 96, 81, 55, 32 and 24 min respectively with respect to increasing humidified feed gas flow rate. These values are close to the corresponding values for 90 vol% aMDEA solution. The curves in each of the Figs. 2–4 give a useful indication of the amount of CO_2 uptake; by integrating the area under the curve and subtracting it from the total area, one can provide the CO_2 sorption capacities of all the above experiments calculated from the CO_2 breakthrough curves.

The behaviors observed in Figs. 2–4 reflect both differences in the rate of CO_2 absorption and the rate of CO_2 stripping. It is useful to compare the rates of absorption and the rates of stripping. Unless the rate of stripping can be enhanced vis-à-vis the rate of absorption, the breakthrough time cannot be increased. For steady state operation, both rates have to be matched; the breakthrough does not arise under such conditions. It is obvious that the rate of stripping was insufficient in these experiments due to a variety of reasons including insufficient stripping membrane module area. As a result, we had feed gas breakthroughs.

Plots of the rates of CO_2 absorption and the CO_2 stripping rates are shown in Fig. 5 against humidified feed gas flow rates in the range of 50–300 cm^3/min for aMDEA absorbent compositions of 80 vol%, 90 vol % and pure aMDEA at three different absorbent flow rates. It is clear that the rate of stripping is highest for pure aMDEA absorbent vis-à-vis the other two absorbent compositions at all three liquid flow rates at the highest feed gas flow rate. The highest rate of stripping achieved was around 18.5 cm^3/min for a feed gas flow rate of 300 cm^3/min. On the other hand, the rate of CO_2 stripping was quite low (in fact, lowest) for 80% aMDEA absorbent composition. This supports our contention that absence of water in pure aMDEA absorbent facilitates stripping other conditions remaining constant. Although there may be some residual water left in the CO_2-loaded absorbent due to absorption from flue gas saturated with moisture, much of it will be utilized during absorption. When the loaded absorbent is heated for stripping, the free water will be gone first; that will facilitate the reverse reaction in Eq. (1). This advantage of enhanced stripping is lost when the fresh absorbent has significant amount of water to start with as in the case of 80% and 90% aMDEA solutions.

To be noted is that the stripping temperature was around 92 °C for pure aMDEA and 90% aMDEA solution in water. Lower temperature stripping is energy-efficient since it uses lower quality heat supply to heat the loaded absorbent. There is an additional advantage here in that during stripping the inevitable evaporation of water which requires

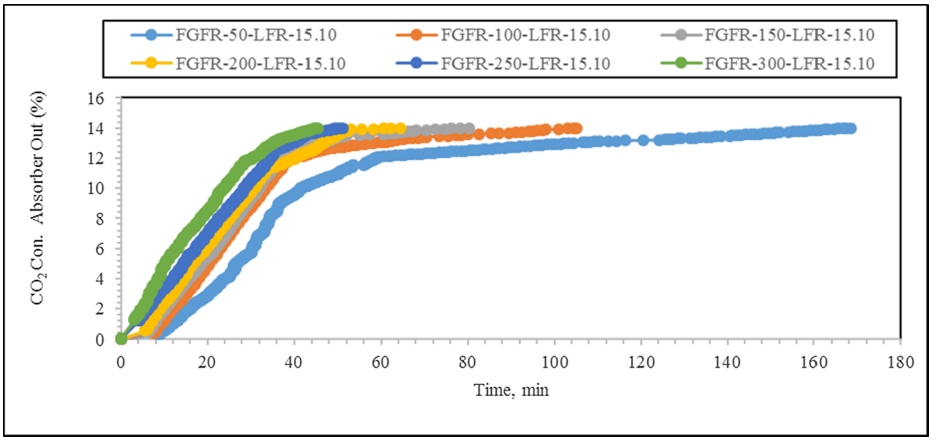

Fig. 3. CO_2 breakthrough results for humidified feed gas flow rates of 50–300 cm^3/min and absorbent concentration of 90 vol% aMDEA at 15.10 L/h; the stripping mode: Sweep He at 50 cm^3/min and vacuum at 1 in Hg (2.54 cm Hg).

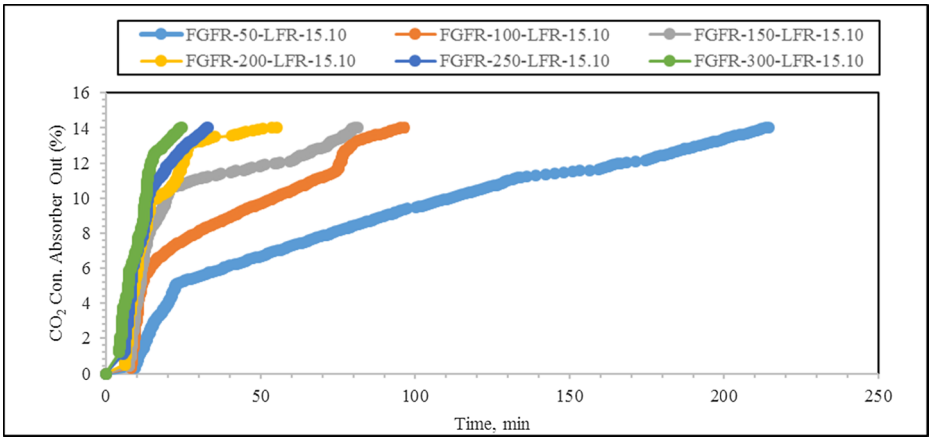

Fig. 4. CO_2 breakthrough results for humidified feed gas flow rates of 50–300 cm^3/min and pure aMDEA absorbent at 15.10 L/h; absorption temperature: 44.6 °C; stripping temperature: 92.7 °C; stripping mode: Sweep He at 50 cm^3/min and vacuum at 1 in Hg (2.54 cm Hg).

considerable latent heat is not needed with pure aMDEA. Extra heat for evaporation will be needed only for the amount of water vapor absorbed from the flue gas which is not used for reaction.

For the conditions providing the highest rate of stripping at the highest feed gas flow rate of 300 cm^3/min for pure aMDEA absorbent, the rate of CO_2 absorption was a high value of 38.6 cm^3/min which works out to more than 90% of the CO_2 present in the feed gas. The rates of CO_2 absorption were close to this value at the other two absorbent compositions as well for this highest feed gas flow rate. However, the rates of absorption were considerably reduced as the feed gas flow rate was reduced. This is due to the fact that at higher feed flue gas flow rates, CO_2 concentration exposed to the absorbent is higher which leads to a higher rate of absorption.

Correspondingly, since the rate of absorption is much reduced at lower feed gas flow rates, the rate of stripping comes close to the rate of absorption. As a result, the breakthrough times are highest in each of the Figs. 2–4 for the lowest feed gas flow rate.

Some of these observations are supported by the plots of percent CO_2 recovered in the stripped gas as a fraction of that absorbed and the rate of CO_2 stripping shown in Fig. 6 for various conditions of operation. An important observation here is as follows. For the 80% aMDEA solution (Fig. 6A, B), the variation of percent CO_2 recovery as a function of feed flue gas flow rate correlates very strongly with the rate of CO_2 stripping; as the feed flue gas flow rate increases, both decrease ultimately flattening out at around 200 cm^3/min +. However, this correlation does not appear to hold for the 90% aMDEA solution in that the rate of stripping does not decrease with an increase in feed flue gas flow rate; rather it increases a bit and essentially flattens out afterwards (Fig. 6C, D). For the pure aMDEA solution (Fig. 6E, F), this departure is enhanced considerably in that the rate of stripping keeps on increasing with an increase in feed flue gas flow rate while the % CO_2 recovery drops but not as much as in the others. Further, the % CO_2 recovery at the highest feed flue gas flow rate is the highest along with the highest rate of stripping.

4. Mass transfer coefficients in membrane contactors

4.1. Overall mass transfer coefficient for the absorber module

The flux of CO_2 through the membrane is affected by various factors, such as the liquid film mass transfer coefficient, gas film mass transfer coefficient, porosity of the hollow fiber membrane, absorption temperature and chemical kinetics in the case of a reactive solvent. The molar CO_2 flux was calculated from the following equation [19,28,29] based on the inlet and outlet gas concentrations of CO_2, inlet gas flow rate (Q_g) and the membrane area (A_m):

$$N_{CO_2} = \frac{Q_g(C_{CO_{2,g,in}} - C_{CO_{2,g,out}})}{A_m} \quad (2)$$

The overall gas phase based mass-transfer coefficient (MTC), K_{og}, for the experimentally obtained molar CO_2 concentrations at a total pressure P_t can be obtained from

$$N_{CO_2} = K_{og}\frac{\Delta y_{lm} P_t}{RT} \quad (3)$$

where the logarithmic mean gas phase CO_2 mole fraction Δy_{lm} is defined by

$$\Delta y_{lm} = \frac{(y_{CO_{2,g,in}} - y^*_{in}) - (y_{CO_{2,g,out}} - y^*_{out})}{In((y_{CO_{2,g,in}} - y^*_{in})/(y_{CO_{2,g,out}} - y^*_{out}))} \quad (4)$$

Here y^*_{in} and y^*_{out} indicate hypothetical gas phase mole fractions in equilibrium with the liquid phase at the two ends of the module and $y_{CO_{2,g,in}}$ and $y_{CO_{2,g,out}}$ indicate the CO_2 mole-fractions of the inlet and outlet gas, respectively.

Since CO_2 reaction with amines is a fast pseudo first order reaction, the mass transfer coefficient does not depend on the liquid film thickness. Further, the values of y^*_{in} and y^*_{out} at the gas-liquid interface is almost negligible; on the other hand, the gas film thickness is likely to have an effect on the CO_2 flux [19,29]. The overall gas-phase-based mass transfer coefficient and volumetric mass transfer coefficient have been calculated using the inlet and the outlet mole fractions of CO_2 obtained from the experimental studies. As shown in Fig. 7, the overall gas phase-based mass transfer coefficient was determined for the following range of operating conditions used e.g., humidified feed gas flow rate in the range of 50–300 cm^3/min, aMDEA absorbent composition of 80 vol%, 90 vol% and pure, liquid flow rate in the range of 15.10–18.90 L/h, for a sweep He flow rate of 50 cm^3/min and vacuum on sweep side 1 in. Hg. The gas phase-based overall mass transfer coefficient increased with increasing humidified feed gas flow rate for all operating conditions studied. Table S1 provides the numerical values of the overall mass transfer coefficient values for humidified feed gas flow rates in the range of 50–300 cm^3/min and liquid absorbent flow rates in the range of 15.10–18.90 L/h for three different aMDEA concentrations (80%, 90% and pure). In general, we observe: (i) an increase in humidified feed gas flow rate increases overall MTC for all conditions; (ii) an increase in liquid absorbent concentration increases overall MTC for the same liquid and gas flow rates. The MTCs were measured during first 5 min.

For a comparison, Cao et al. [4] obtained overall mass transfer coefficient values of 1.0×10^{-4} ms^{-1}, 1.9×10^{-4} ms^{-1}, 2.0×10^{-4} ms^{-1} and 2.1×10^{-4} ms^{-1}, for liquid flow rates of 0.01 ms^{-1}, 0.03 ms^{-1}, 0.06 ms^{-1}, 0.09 ms^{-1}, respectively under conditions with

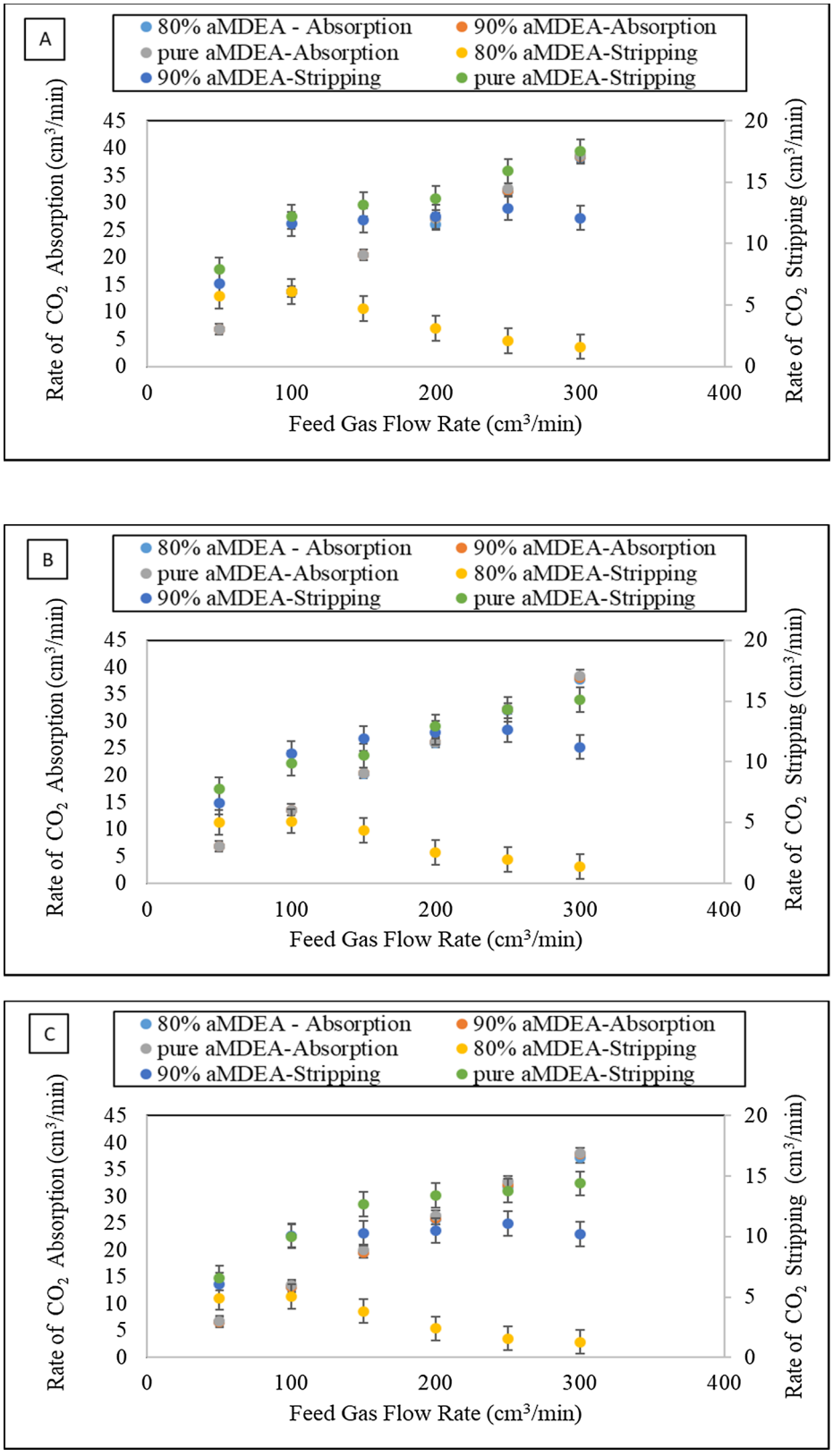

Fig. 5. CO_2 absorption/stripping rates achieved at three different absorbent compositions for LFRs of (A) 15.10 L/h, (B) 16.60 L/h and (C) 18.90 L/h. Sweep He flow rate was 50 cm^3/min and vacuum on sweep side was 1 in. NOTE: Orange symbols are for 90% aMDEA absorption. These values are very close to the values for pure aMDEA absorption and overlap with those values and are not very visible. (For interpretation of the references to colour in this figure legend, the reader is referred to the web version of this article.)

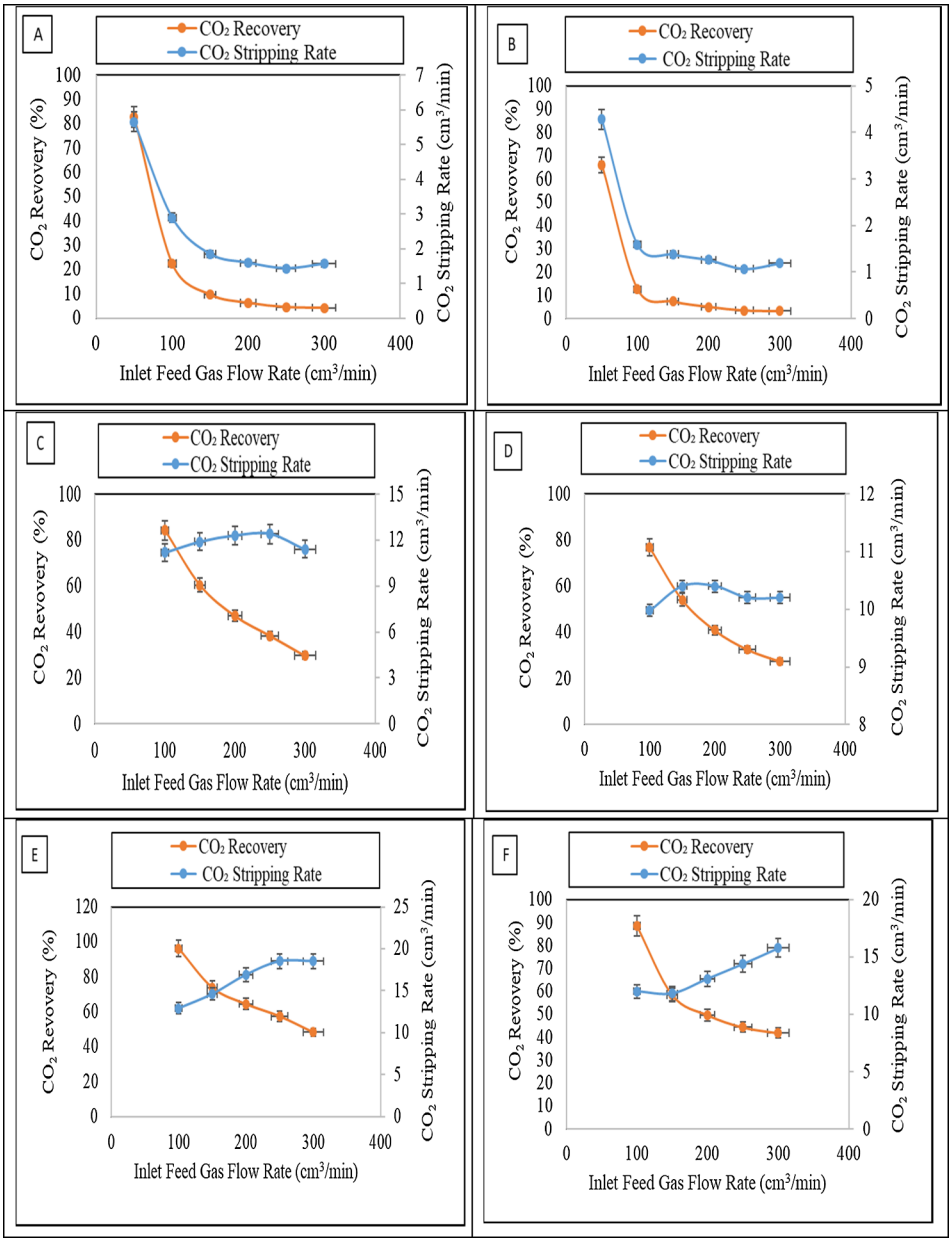

Fig. 6. Percent CO_2 recovery and CO_2 stripping rate for (A) 80% aMDEA at LFR of 15.10 L/h, (B) 80% aMDEA at LFR of 18.90 L/h, (C) 90% aMDEA at LFR of 15.10 L/h, (D) 90% aMDEA at LFR of 18.90 L/h, (E) pure aMDEA at LFR of 15.10 L/h, and (F) pure aMDEA at LFR of 18.90 L/h. In all cases, He flow rate was 100 cm^3/min and vacuum on sweep side was 2.54 cm Hg.

amine concentration of 2 mol/L in water, feed gas containing 20% v/v CO_2 and gas velocity of 3000 cm^3/min using MDEA tertiary amine solution at room temperature in a PTFE hollow fiber-based membrane contactor. It is clear that the overall mass transfer coefficient obtained in the present study is higher than these values, although our gas flow rate is much lower along with a lower CO_2 concentration in the incoming feed gas. It is a well-known fact that gas flow rate plays an important role in CO_2 absorption process in enhancing the overall mass transfer coefficient because gas velocity results in the enhancement of driving force which can improve the mass transfer performance for CO_2 absorption with amine solutions.

Lin et al. [30] have investigated CO_2 absorption in PVDF and PP membrane contactors using mixed absorbent including 2-amino-2-methyl-1-propanol (AMP) + PZ and MDEA + PZ. They also found a similar behavior in that the overall mass transfer coefficient increased with an increase of gas flow rate [30]. However, despite this fact, the reason for higher overall MTC in case of higher gas flow rate can be explained as the usage of activated MDEA providing fast reaction with CO_2 and so higher absorption capacity and mass transfer can be observed.

4.2. Overall volumetric mass transfer coefficient for the absorber module

The overall volumetric mass transfer coefficient for absorbent aMDEA with 80% concentration increased from 0.085 s^{-1} in case of maximum liquid flow rate (18.90 L/h), sweep He flow rate (100 cm^3/min) and minimum humidified feed gas flow rate (50 cm^3/min) to 0.484 s^{-1} in case of liquid flow rate of 15.10 L/h, sweep He flow rate of 50 cm^3/min and humidified feed gas flow rate of 300 cm^3/min. The maximum volumetric mass transfer coefficient for 80% absorbent concentration is more than six times greater than the highest volumetric mass transfer coefficient in a packed column, a conventional technique used in gas separation (0.075 s^{-1}) [18,31]. The maximum overall volumetric gas phase-based mass transfer coefficient ($K_{og}a_v$) for the

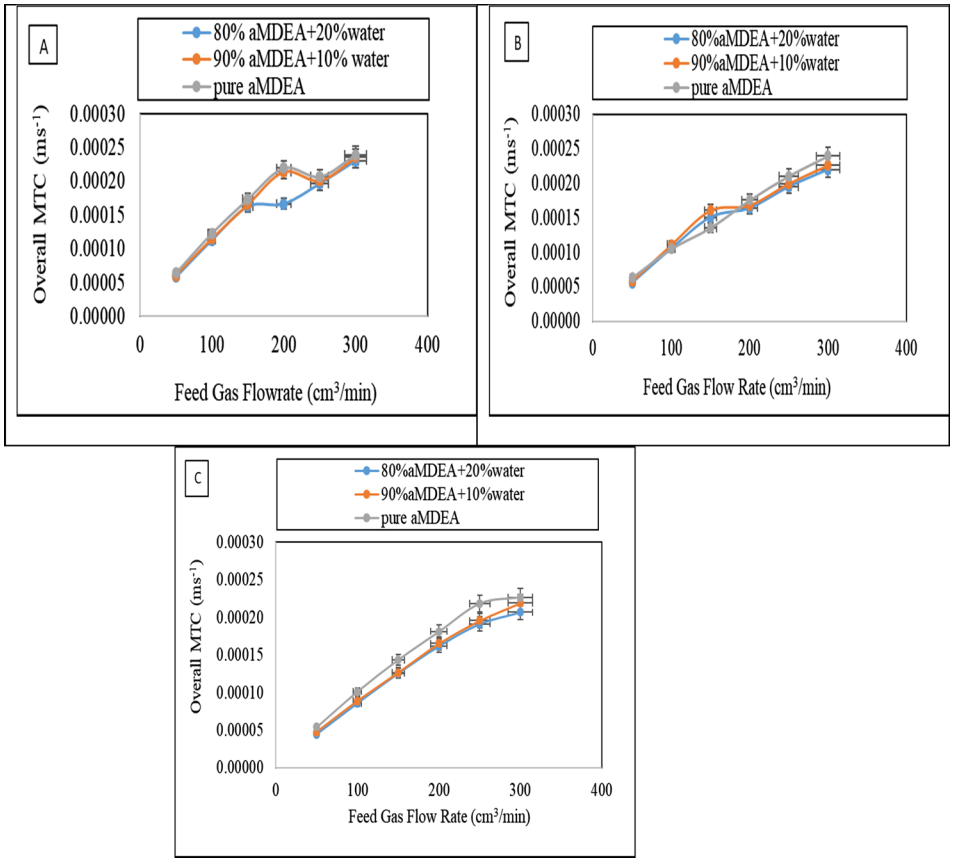

Fig. 7. Overall mass transfer coefficient as a function of the humidified feed gas flow rate in the cases of three different absorbent compositions and three LFRs, (A) 15.10 L/h, (B) 16.60 L/h and (C) 18.90 L/h.

current study is 0.504 s^{-1} for pure aMDEA absorbent in case of liquid flow rate of 15.10 L/h and sweep He flow rate of 50 cm^3/min. The $K_{og}a_v$ reported by Li et al. [18] using poly(ether ether ketone) (PEEK) hollow fiber membrane modules to capture CO_2 from flue gas [18] for both 40 wt% aMDEA and 50 wt% aMDEA absorbents is 1.5 s^{-1}. These comparisons are provided in Table 2.

The data in Li et al. [18] were obtained for larger cylindrical modules of 4 in and 8 in diameter. The type of hollow fiber membrane module used here have been used in larger-scale devices for a different separation process namely, membrane distillation. For example, Song et al. [32] used rectangular modules having designs similar to here with one module having as much surface area as 0.67 m^2; they had used a total of ten modules in their pilot plant studies. Cylindrical modules have also been developed by Singh et al. [33] with an individual module having a surface area of 0.6 m^2; such a module can be easily scaled up to a diameter of 4 to 8 in.

5. Considerations on energy requirements vis-à-vis stripping

Among various cost elements responsible for the high energy consumption in CO_2 absorption-stripping processes, stripping is highly energy intensive. In MEA-based processes, stripping conditions are around 110–120 °C at ~2 atm [17]. Many efforts are being directed at reducing this cost; see recent examples [34,35]. For stripping CO_2 from an aqueous aMDEA solution using a membrane desorber, conditions employed were (Li et al., [18]): Solvents aMDEA/H_2O (40 wt%); Liquid flow rate 1–2 L/min; solvent flash vessel temperature 104–122 °C; solvent flash vessel pressure 40–55 psig; solvent pressure drop across the membrane 40 psig. In this study, we have shown that at around 90 °C, we can get considerable stripping using pure aMDEA as absorbent. This has a number of beneficial features in terms of thermal input reduction such as reduced absorbent mass to be heated, no thermal energy to be spent in evaporating free water added to start with. However, we had used here a small sweep gas flow rate as well as vacuum in the combo mode on the permeate side of the stripper. We need to explore whether pressurizing the feed solution on one side of the membrane stripper with somewhat smaller membrane pore size will achieve adequate stripping with appropriate allowance for higher membrane area than that in the membrane absorber.

5.1. Membrane surface coating

A SEM of the surface of the coated hollow fibers used in the stripping module is shown in Fig. 8. Anyone familiar with the well-known base Celgard® hollow fibers will immediately recognize that the slit-like, sub-micron pore surfaces now appear quite hazy due to the polymer grafting. The fluorosiloxane coating is quite inert. Further, the coating appears everywhere protecting the base PP polymer from continuous contact with amine solvent. A thicker coating with even further reduced pore size may be needed if the feed solution is pressurized during stripping.

Table 2
Comparison of K_g a_v.

Solvent	Interfacial area a_v (m^2/m^3)	$K_g a_v$ (s^{-1})
40 wt% aMDEA[18]	1198	1.5
50 wt% aMDEA[18]	1198	1.5
Pure aMDEA (this work)	2100	0.504

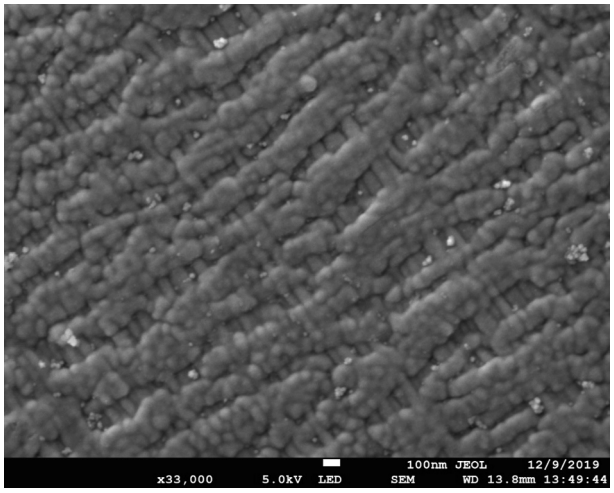

Fig. 8. SEM photo of the surface of the coated hollow fiber in the stripping module.

6. Concluding remarks

Experimental studies were carried out successfully to absorb CO_2 from simulated wet flue gas into pure organic absorbent of aMDEA in a hollow fiber membrane contactor at temperatures in the range of 25–45 °C. Other absorbents used were aqueous aMDEA solutions having 10% and 20% water. Stripping of CO_2 from the CO_2-loaded absorbent was carried out at temperatures ~ 92 °C in an almost identical membrane contactor functioning as a stripper with the help of a sweep gas and vacuum. The membrane contactors employed porous polypropylene hollow fibers having a porous plasma polymerized fluorosiloxane coating on the outside surface. The absorbent was in cross-flow in both the absorber and the stripper.

Using pure aMDEA absorbent, we were able to absorb as much as 90%+ of CO_2 from a feed gas flow rate of 300 cm^3/min in a module having 509 cm^2 membrane surface area; other high aMDEA-containing aqueous absorbents achieved a similar rate of CO_2 absorption. However, the rate of CO_2 stripping achieved was highest with pure aMDEA absorbent; further, this rate was considerably higher than those achieved with the other aqueous aMDEA-based absorbent solutions. This demonstrates that pure aMDEA is a much better candidate for use as CO_2 absorption solvent for the following reasons: lower temperature of stripping which requires lower quality heat; absence of excess water and consequent advantages in MDEA-based reverse reaction; drastic reduction in the circulating absorbent flow rate from the usual 30–50% aqueous solution of the reactive amine absorbent and therefore a substantial reduction in the amount of energy used to heat up the CO_2-loaded absorbent.

The volumetric overall mass transfer coefficient achieved with pure aMDEA during CO_2 absorption was a high value of 0.504 sec^{-1} for a module interfacial area per unit volume of 2100 m^{-1}. Increased feed flow rate increased overall mass transfer coefficient. The stripping process at lower temperatures used here was slower. Matching of absorption and stripping rates requires that the stripper surface area is increased. Exploration of pressurized mode of stripping to eliminate the use of vacuum and sweep gas and enhance stripping is suggested.

Declaration of Competing Interest

The authors declare that they have no known competing financial interests or personal relationships that could have appeared to influence the work reported in this paper.

Acknowledgements

This study is based on the first author's PhD thesis, which was carried out under the third author's co-supervision at New Jersey Institute of Technology (NJIT), Department of Chemical and Materials Engineering, Newark, NJ, USA. Aytac Perihan Akan was financially supported by The Scientific and Technological Research Council of Turkey (TUBITAK) with 2214A-fellowship to implement her studies at NJIT, USA.

Appendix A

See Table S1.

Table S1
Gas phase based overall mass transfer coefficient.*

Gas phase based overall mass transfer coefficient (MTC), K_{og}, (ms^{-1})										
		Liquid absorbent concentration								
		80% aMDEA + 20% water			90% aMDEA + 10% water			Pure aMDEA		
		Liquid flow rate (L/h)			Liquid flow rate (L/h)			Liquid flow rate (L/h)		
		15.10	16.60	18.90	15.10	16.60	18.90	15.10	16.60	18.90
Humidified feed gas flow rate (cm^3/min)	50	5.82×10^{-5}	5.56×10^{-5}	4.49×10^{-5}	6.04×10^{-5}	5.78×10^{-5}	4.79×10^{-5}	6.29×10^{-5}	6.04×10^{-5}	5.42×10^{-5}
	100	1.13×10^{-4}	1.05×10^{-4}	8.61×10^{-5}	1.15×10^{-4}	1.11×10^{-4}	8.91×10^{-5}	1.23×10^{-4}	1.15×10^{-4}	1.01×10^{-4}
	150	1.63×10^{-4}	1.51×10^{-4}	1.26×10^{-4}	1.66×10^{-4}	1.61×10^{-4}	1.27×10^{-4}	1.73×10^{-4}	1.65×10^{-4}	1.44×10^{-4}
	200	1.67×10^{-4}	1.64×10^{-4}	1.62×10^{-4}	2.14×10^{-4}	1.68×10^{-4}	1.65×10^{-4}	2.19×10^{-4}	1.72×10^{-4}	1.81×10^{-4}
	250	1.97×10^{-4}	1.95×10^{-4}	1.91×10^{-4}	2.01×10^{-4}	1.99×10^{-4}	1.96×10^{-4}	2.07×10^{-4}	2.03×10^{-4}	2.19×10^{-4}
	300	2.31×10^{-4}	2.20×10^{-4}	2.07×10^{-4}	2.36×10^{-4}	2.26×10^{-4}	2.19×10^{-4}	2.40×10^{-4}	2.36×10^{-4}	2.27×10^{-4}

* Sweep He flow rate at 50 cm^3/min; vacuum on sweep side 1 in. Hg (2.54 cm Hg).

References

[1] H. Yang, Z. Xu, M. Fan, R. Gupta, R.B. Slimane, A.E. Bland, I. Wright, Progress in carbon dioxide separation and capture: A review, J. Environ. Sci. 20 (2008) 14–27, https://doi.org/10.1016/S1001-0742(08)60002-9.

[2] M.R.M. Abu-Zahra, L.H.J. Schneiders, J.P.M. Niederer, H.M.P. Feron, G.F. Versteeg, CO_2 capture from power plants Part I. a parametric study of the technical performance based on monoethanolamine, Int. J. Greenh. Gas Con. 1 (2007) 37–46, https://doi.org/10.1016/S1750-5836(06)00007-7.

[3] A.A. Olajire, CO_2 capture and separation technologies for end-of-pipe applications-A review, Energy 35 (2010) 2610–2628.

[4] F. Cao, G. Gao, H. Gao, H. Zhang, Z. Liang, R. Idem, P. Tontiwachwuthikul, Investigation of mass transfer coefficient of CO_2 absorption into amine solutions in hollow fiber membrane contactor, Energy Procedia 114 (2017) 621–626, https://doi.org/10.1016/j.egypro.2017.03.1204.

[5] M.H. Ibrahim, M.H. El-Naas, Z. Zhang, B. Van der Bruggen, CO_2 capture using hollow fiber membranes: a review of membrane wetting, Energ. Fuel 32 (2018) 963–978, https://doi.org/10.1021/acs.energyfuels.7b03493.

[6] C. Song, Q. Liu, N. Ji, S. Deng, J. Zhao, Y. Li, Y. Song, H. Li, Alternative pathways for efficient CO_2 capture by hybrid processes – A review, Renew. Sust. Energy. Rev. 82 (2018) 215–231, https://doi.org/10.1016/j.rser.2017.09.040.

[7] Y. Wang, L. Zhao, A. Otto, M. Robinius, D. Stolten, A review of post-combustion CO_2 capture technologies from coal-fired power plants, Energy Procedia 114 (2017) 650–665, https://doi.org/10.1016/j.egypro.2017.03.1209.

[8] A. Brunetti, F. Scura, G. Barbieri, E. Drioli, Membrane technologies for CO_2 separation, J. Membr. Sci. 359 (2010) 115–125, https://doi.org/10.1016/j.memsci.2009.11.040.

[9] J. Luis Míguez, J. Porteiro, R. Pérez-Orozco, D. Patiño, S. Rodríguez, Evolution of CO_2 capture technology between 2007 and 2017 through the study of patent activity, Appl. Energ. 211 (2018) 1282–1296, https://doi.org/10.1016/j.apenergy.2017.11.107.

[10] Y. Labreche, Functionalized polymeric membranes for CO_2 capture, J. Membr. Sci. Res. 2 (2016) 59–65, https://doi.org/10.22079/JMSR.2016.19153.

[11] A. Xu, A. Yang, S. Young, D. deMontigny, P. Tontiwachwuthikul, Effect of internal coagulant on effectiveness of polyvinylidene fluoride membrane for carbon dioxide separation and absorption, J. Membr. Sci. 311 (2008) 153–158, https://doi.org/10.1016/j.memsci.2007.12.008.

[12] T. Kuramochi, A. Ramírez, W. Turkenburg, A. Faaij, Comparative assessment of CO_2 capture technologies for carbon-intensive industrial processes, Prog. Energy Combust. 38 (2012) 87–112, https://doi.org/10.1016/j.pecs.2011.05.001.

[13] C.E. Powell, G.G. Qiao, Polymeric CO_2/N_2 gas separation membranes for the capture of carbon dioxide from power plant flue gases, J. Membr. Sci. 279 (2006) 1–49, https://doi.org/10.1016/j.memsci.2005.12.062.

[14] I. Iliuta, F. Bougie, M.C. Iliuta, CO_2 removal by single and mixed amines in a hollow-fiber membrane module-investigation of contactor performance, AIChE J. 61 (2015) 955–971, https://doi.org/10.1002/aic.14678.

[15] P. Luis, B. Van der Bruggen, The role of membranes in post-combustion CO_2 capture, Greenh. Gases 3 (2013) 1–20, https://doi.org/10.1002/ghg.1365.

[16] A. Mansourizadeh, A.F. Ismail, Hollow fiber gas-liquid membrane contactors for acid gas capture: A review, J. Hazard. Mater. 171 (2009) 38–53, https://doi.org/10.1016/j.jhazmat.2009.06.026.

[17] G.T. Rochelle, Amine scrubbing for CO_2 capture, Science 325 (2009) 1652–1654, https://doi.org/10.1126/science.1176731.

[18] S. Li, T.J. Pyrzynski, N.B. Klinghoffer, T. Tamale, Y. Zhong, J.L. Aderhold, S.J. Zhou, H.S. Meyer, Y. Ding, B. Bikson, Scale-up of PEEK hollow fiber membrane contactor for post-combustion CO_2 capture, J. Membr. Sci. 527 (2017) 92–101, https://doi.org/10.1016/j.memsci.2017.01.014.

[19] T. Mulukutla, G. Obuskovic, K.K. Sirkar, Novel scrubbing system for post-combustion CO2 capture and recovery: Experimental studies, J. Membr. Sci. 471 (2014) 16–26, https://doi.org/10.1016/j.memsci.2014.07.037.

[20] T.L. Donaldson, Y.N. Nguyen, Carbon dioxide reaction kinetics and transport in aqueous amine membranes, Ind. Eng. Chem. Fund. 19 (1980) 260–266, https://doi.org/10.1021/i160075a005.

[21] F. Cao, H. Gao, Q. Xiong, Z. Liang, Experimental studies on mass transfer performance for CO_2 absorption into aqueous N, N-dimethylethanolamine (MDEA) based solutions in a PTFE hollow fiber membrane contactor, Int. J. Greenh. Gas Con. 82 (2019) 210–217, https://doi.org/10.1016/j.ijggc.2018.12.011.

[22] S. Bishnoi, G.T. Rochelle, Absorption of carbon dioxide in aqueous piperazine/methyldiethanolamine, AlChE J. 48 (2002) 2788–2799, https://doi.org/10.1002/aic.690481208.

[23] J. Lu, L. Wang, X. Sun, J. Li, X. Liu, Absorption of CO_2 into aqueous solutions of methyldiethanolamine and activated methyldiethanolamine from a gas mixture in a hollow fiber contactor, I&EC Res. 44 (2005) 9230–9238, https://doi.org/10.1021/ie058023f.

[24] P.W.J. Derks, Carbon dioxide absorption in piperazine activated N-Methlydiethanolamie, PhD. Thesis, University of Twente, The Netherlands, 2006.

[25] H. Svensson, C. Hulteberg, H.T. Karlsson, Heat of absorption of CO_2 in aqueous solutions of N-methyldiethanolamine and piperazine, Int. J. Greenh. Gas Con. 17 (2013) 89–98, https://doi.org/10.1016/j.ijggc.2013.04.021.

[26] M. Saidi, Process assessment and sensitivity analysis of CO_2 capture by aqueous methyldiethanolamine + piperazine blended solutions using membrane contactor: Model development of kinetics and mass transfer rate, Sep. Purif. Technol. 204 (2018) 185–195, https://doi.org/10.1016/j.seppur.2018.04.063.

[27] G.W. Xu, C.F. Zhang, S.J. Qin, W.H. Gao, H.B. Liu, Gas-liquid equilibrium in a CO_2-MDEA-H_2O system and the effect of piperazine on it, Ind. Eng. Chem. Res. 37 (1998) 1473–1477, https://doi.org/10.1021/ie9506328.

[28] P.H.M. Feron, A.E. Jansen, CO_2 separation with polyolefin membrane contactors and dedicated absorption liquids: performances and prospects, Sep. Purif. Technol. 27 (2002) 231–242, https://doi.org/10.1016/S1383-5866(01)00207-6.

[29] K.K. Sirkar, Separation of Molecules, Macromolecules and Particles: Principles, Phenomena and Processes, Cambridge University Press, New York, 2014.

[30] S.H. Lin, P.C. Chiang, C.F. Hsieh, M.H. Li, K.L. Tung, Absorption of carbon dioxide by the absorbent composed of piperazine and 2-amino-2-methyl-1-propanol in PVDF membrane contactor, J. Chin. Inst. Chem. Eng. 39 (2008) 13–21, https://doi.org/10.1016/j.jcice.2007.11.010.

[31] B.W. Reed, M.J. Semmens, E.L. Cussler, Membrane contactors, in: R.D. Noble, S.A. Stern (Eds.), Membrane Separation Technology: Principles and Applications, Elsevier Science, 1995, pp. 467–478.

[32] L. Song, Z. Ma, X. Liao, P.B. Kosaraju, J.R. Irish, K.K. Sirkar, Pilot plant studies of novel membranes and devices for direct contact membrane distillation-based desalination, J. Membr. Sci. 323 (2008) 257–270, https://doi.org/10.1016/j.memsci.2008.05.079.

[33] D. Singh, L. Li, G. Obusckovic, J. Chau, K.K. Sirkar, Novel cylindrical cross-flow hollow fiber membrane module for direct contact membrane distillation-based desalination, J. Membr. Sci. 545 (2018) 312–322, https://doi.org/10.1016/j.memsci.2017.09.007.

[34] S. Yan, Q. Cui, L. Xu, T. Tu, Q. He, Reducing CO_2 regeneration heat requirement through waste heat recovery from hot stripping gas using nanoporous ceramic membrane, Int. J. Greenh. Gas Con. 82 (2019) 269–280, https://doi.org/10.1016/j.ijggc.2019.01.017.

[35] C.A. Scholes, S.E. Kentish, G.W. Stevens, J. Jin, D. deMontigny, Thin-film composite membrane contactors for desorption of CO_2 from Monoethanolamine at elevated temperatures, Sep. Purif. Technol. 156 (2015) 841–847, https://doi.org/10.1016/j.seppur.2015.11.010.